Electromechanical Transient Modeling of Fast Electric Vehicle Charging Unit

Shuyao Wang[1], Haiguo Li[1], Yiwei Ma[1], Fred Wang[1,2] and Leon M. Tolbert[1,2]
[1]The University of Tennessee, [2]Oak Ridge National Laboratory
Knoxville, TN 37996-2250, USA
swang67@vols.utk.edu; hli96@vols.utk.edu; yma13@vols.utk.edu; fred.wang@utk.edu; tolbert@utk.edu

***Abstract*—Fast electric vehicle (EV) charging stations have become one of the fastest-growing penetrated power electronics (PE) interfaced loads to the electric power system. The lack of accurate model of the fast EV charger in transient stability (TS) simulation tools limits the effectiveness of power system dynamic performance evaluation and stability analysis. In this paper, The electromechanical model of a fast EV charging unit is proposed, which is suitable for large-scale power system dynamic analysis in TS simulators. The EV charger model is simplified to guarantee a balance between model accuracy and simplicity. The validity of the proposed model has been demonstrated by a comparative study with the benchmark model created in PSCAD/EMTDC.**

***Index Terms*—electromechanical modeling, electric vehicle fast charging, TSAT, PSCAD/EMTDC, transient stability**

I. Introduction

Power electronics (PE) interfaced loads have become one of the most common types in the electric power system. They range from high-power-rating applications, *e.g.,* fast electric vehicle (EV) charging stations, to low-power-rating appliances, *e.g.,* consumer chargers, and among which, the DC fast EV charging stations have increasingly penetrated into the power grid [1]. Moreover, the fast EV charger is a typical nonlinear load with high power consumption, which affects the grid transient stability (TS) when integrated into the conventional ac network [2]. Therefore, it is of great importance to investigate the dynamic performance of fast EV charging load.

Load models are classified as static models and dynamic models in the TS analysis. According to the survey on the international industry load modeling practice conducted by CIGRE (International Council on Large Electric Systems) in 2013, the PE interfaced load is mostly represented by the static load in the TS analysis [3], [4]. However, applying the dynamic model of PE interfaced load to the TS simulators will promote the accuracy of the TS analysis since the static model cannot fully characterize the load dynamics, especially considering system transients.

Although the dynamic performance of EV charging units has been widely modeled and analyzed in electromagnetic transient (EMT) simulators, such as PSCAD/EMTDC [5], it is critical to develop the dynamic EV charger model that is adaptive to TS simulation tools. It is because the short simulation time step in the EMT simulator computationally prohibits the study of the large-scale transmission network. Comparatively speaking, the TS simulator, which focuses on the electromechanical transients and oscillations between 0.1 $\sim$ 3 Hz [6], is more suitable for large-scale network simulation analysis.

According to existing investigations, the dynamic PE interfaced load model can be classified as 1) equivalent circuit model, which includes the detailed and the average equivalent model [7]–[9]. The equivalent circuit model is complicated for TS simulators since it features the load circuit topology; 2) general state-space model, where the load electrical component and control strategy are described by differential equations. State-space models are more suitable to be used in TS simulations compared with equivalent circuit models, but reasonable simplification is required considering the accessibility to the large-scale network simulation. Some other PE interfaced devices, including both electric sources and load, have been modeled by this approach, *e.g.,* the PE-based variable speed drive (VSD) modeled in the commercial TS simulation software are proposed in [10]–[13], the model of photovoltaic (PV) generation resources and battery energy storage system (BESS) have been proposed and adopted by commercial software [14]–[16].

However, the EV fast charging unit modeled by this approach has not been sufficiently studied to the best of the authors' knowledge. In the limited literature that has proposed the dynamic model of EV charger, the application in the TS simulator is rarely mentioned, *e.g.,* in [17] the state-space model based EV charging unit is developed for voltage stability analysis without considering the dynamics of charger controller and battery load. Furthermore, the modeling of fast EV charging unit is different from the above PE based devices in the following aspects: 1) the EV charging units have different control scheme and physical configuration compared with VSD loads; 2) there is no internal induced voltage in EV charging units compared with the PE based PV generators; 3) EV charging units have distinct operation mode that should be specified in the corresponding load model, *e.g.,* the low-voltage ride-through (LVRT).

In this paper, the model of fast EV charging unit is developed in TSAT (Transient Security Assessment Tool) by the user-defined model (UDM) editor. The proposed EV charger model is derived based on the average model of PE devices, which guarantees a balance between the model accuracy and simplicity. Meanwhile, the proposed EV charger model specifies the LVRT capability. The paper is organized as

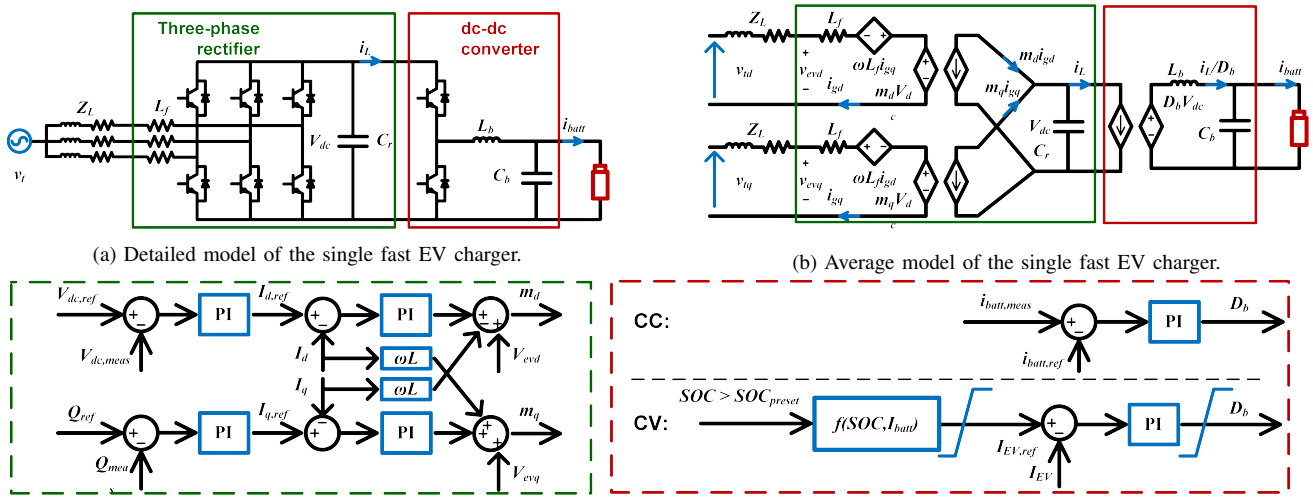

(a) Detailed model of the single fast EV charger.

(b) Average model of the single fast EV charger.

(c) Control scheme of three-phase rectifier and DC-DC converter.

Fig. 1. The circuit diagram and control scheme of fast EV charging unit.

follows: Section II introduces the circuit topology, the control algorithm, and the model simplification principle of the EV charging unit. Section III explains the EV charger model in the TS simulator, which specifies the integration of the equivalent circuit model and the controller model in the phasor domain. Part IV presents the model verification of the EV charger load considering various testing conditions, and conclusions are drawn in section V.

II. EV Charging Unit Dynamic Characterization: Topology and Control

A. EV Charger Detailed and Equivalent Average Model

The circuit topology of the DC fast EV charging unit studied in this paper is illustrated in Fig. 1(a), which includes the terminal AC bus V_t, the charging circuit, and the battery load. Generally, the charging circuit consists of two power stages, one of which is the three-phase active front end rectifier transferring the ac voltage supply to a stable DC voltage, the other is a DC-DC converter regulating the battery charging mode.

The EV charger average model in the dq coordinates is adopted in this paper as the basic circuit configuration since the switching dynamics of PE devices are not considered in the TS analysis. As illustrated in Fig. 1(b), the EV charger dynamic performance of different power stages is characterized by modulation index m_d, m_q and D_b respectively.

The lithium-ion battery expressed by Shepherd model is selected as the battery load model in this paper since it is one of the most frequently used types of battery for the EV [18].

B. Control Schemes of Fast EV Charging Unit

The control schemes of the three-phase rectifier and DC-DC converter are illustrated in Fig. 1(c), which characterize the dynamic performance of the corresponding charging circuit. In this paper, vector control is selected for the three-phase rectifier, which regulates the voltage across the DC-link capacitor C_r and provides unity power factor. The DC-DC converter is regulated as two basic charging modes, the constant current (CC) and constant voltage (CV) mode [9], based on the battery state of charge (SoC).

C. EV Charging Unit LVRT Controller Design

The EV charger is supposed to perform the LVRT for 12 cycles as regulated in [19], or else it may induce a significant voltage swell after the terminal voltage is recovered due to a large amount of load loss. However, the LVRT scheme is not clearly specified according to authors' best knowledge. So an LVRT control is designed and adopted by the fast EV charger studied in this paper to present a more practical load response. The LVRT algorithm adopted in this paper is illustrated in Fig. 2 and expressed in (1):

$$I_{batt,ref} = \begin{cases} I_{batt,ref,nom}, & when \quad V_{mag} > V_{th1} \\ (-V_{th2} + V_{mag})/(V_{th1} - V_{th2}), & when \quad V_{th2} \leq V_{mag} \leq V_{th1} \\ 0, & when \quad V_{mag} < V_{th2} \end{cases} \tag{1}$$

where $I_{batt,ref}$ represents the battery current control reference, $I_{batt,ref,nom}$ represents the current reference at the nominal operating condition, V_{mag} represents the voltage magnitude of V_t, and V_{th1}, V_{th2} represent the threshold voltage of V_{mag}.

D. EV Charging Unit Model Simplification

The following simplification approach is adopted in this paper: 1) The average model is used to characterize the EV charger circuit topology. 2) The battery charging current is supposed to closely follow the $I_{batt,ref}$ considering the high control bandwidth of the DC-DC converter, of which the verification process is not presented here considering the length of the paper. So the battery load and DC-DC converter are regarded as a current source, of which the load current is varied according to the $I_{batt,ref}$. 3) The dynamics of the three-phase rectifier inner current control loop is simplified as

a first-order system due to its high control bandwidth. Detailed information is presented in Section III.

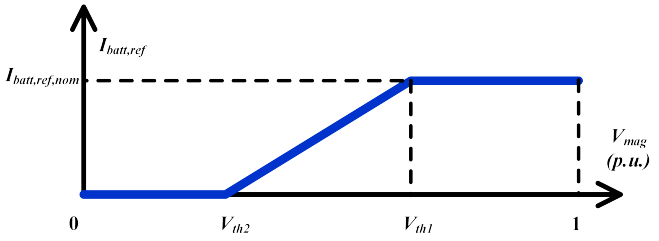

Fig. 2. EV fast charging unit LVRT control scheme.

III. EV Charger Realization in TS Simulator

According to existing studies [20]–[22], the positive-sequence model of PE interfaced devices in the TS simulator is usually divided into the following 3 parts:

- The AC side dynamic model, which includes the point of common coupling (PCC), the decoupling inductance, and the equivalent AC side model which is usually specified as an AC voltage source.
- The DC side dynamic model, which specifies the dynamic performance of the DC energy storage component C_r.
- The dynamic controller model, which characterizes the dynamic performance of the AC and DC side models.

According to Fig. 1(b), the equivalent physical model of the fast EV charger in the TS simulator is illustrated in Fig. 3, which characterizes a combination of the AC and DC side models without a controller specifying the dynamic performance. The V_{ev} and I in Fig. 3 represent the equivalent AC voltage source specifying the EV charger, and the load current at AC side respectively.

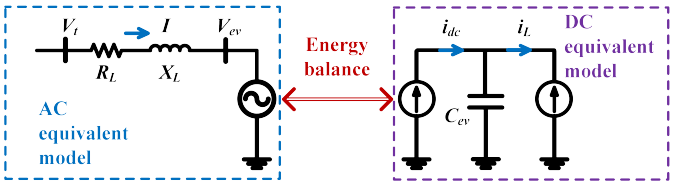

Fig. 3. Equivalent physical model of fast EV charger in TS simulator.

A. Electrical Variables Transformation between TS and EMT

The AC equivalent model of the EV fast charging unit should be represented in the phasor domain considering the TS simulator requirement. Therefore, the transformation between the dq coordinates and the phasor domain is necessary. The phasor domain coordinates, denoted as RI coordinates in the following passage, is illustrated in Fig. 4 by solid black lines, where the real and imaginary axes are used to represent the phase angle and the amplitude of the electrical variables [23]. The corresponding phasor variables remain static at the steady state operating point in the static RI coordinates. The dq axis, which is illustrated by the black dash line in Fig. 4, rotates at the fundamental frequency of the adjacent AC grid. The V and I are illustrated in Fig. 4 as an example of the voltage and current in RI coordinates. In this paper, the PCC voltage V_t is aligned with the d axis, so the transformation from the dq coordinates to the phasor domain is expressed as follows:

$$\begin{aligned} I_R &= \sqrt{i_d^2 + i_q^2} \cdot \cos(\theta_2) \\ I_I &= \sqrt{i_d^2 + i_q^2} \cdot \sin(\theta_2) \end{aligned} \tag{2}$$

$$\begin{aligned} \theta_d &= \theta_2 - \theta_1 = \arctan(i_q/i_d) \\ \theta_2 &= \arctan(V_I/V_R) + \theta_d \end{aligned} \tag{3}$$

where i_d and i_q represent the current I in the dq coordinates; V_R and V_I represent the voltage V in the RI coordinates; I_R and I_I represent I in the RI coordinates; θ_1 and θ_2 represent the V and I phase angle; θ_d represents the angle difference between θ_1 and θ_2.

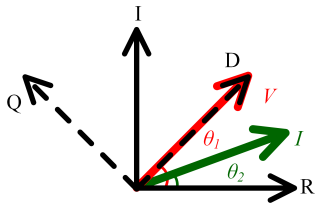

Fig. 4. Reference frame transformation [23].

B. EV Charging Unit AC Terminal Specification

Combining with the DC model and corresponding controllers, the framework of the positive sequence EV charger model proposed in this paper is illustrated in Fig. 5. With the line current I_d and I_q derived by the controller model in Fig. 5, the V_{ev} in phasor domain is expressed as:

$$\dot{V_{ev}} = \dot{V_t} - (R_L + jX_L)\dot{I_{ref}} \tag{4}$$

where $\dot{I_{ref}}$ represents the current flowing through the transmission line derived by the controller model, of which the phasor expression is derived by (2), (3).

IV. EV Fast Charging Unit Model Benchmark

The TS model of the fast EV charging unit is developed in TSAT based on the modeling process presented in section III, and the accuracy of the proposed electromechanical model is verified in this section. As illustrated in Fig. 6, the EV charger model is connected to the IEEE 3-machine 9-bus transmission network at Bus 5. The overall load profile is listed in Table I.

The detailed EMT model of the network above has been developed in the PSCAD/EMTDC as the benchmark model to evaluate the accuracy of the TS model. The transmission line disconnection and three-phase ground fault close/ remote to the EV charger load bus are simulated and analyzed respectively in the following subsections. Meanwhile, the different dynamic performance between the proposed load model and the static model is also specified.

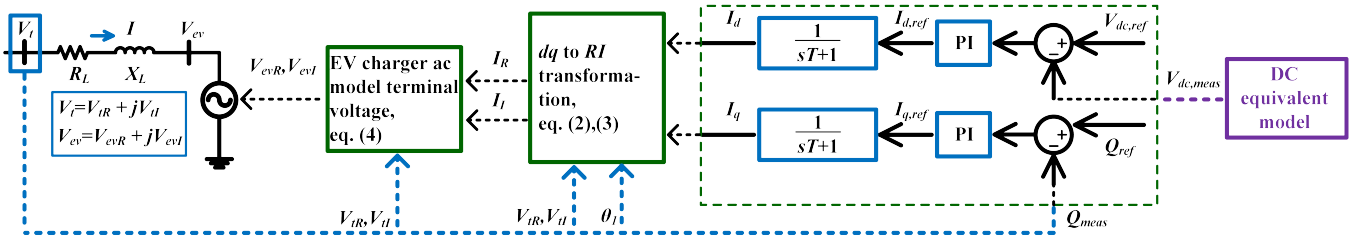

Fig. 5. Framework of the positive-sequence EV charger model in the TS simulator.

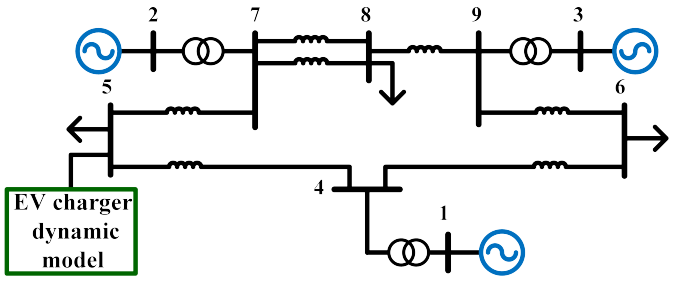

Fig. 6. Fast EV charger integrated into the 3-machine 9-bus system.

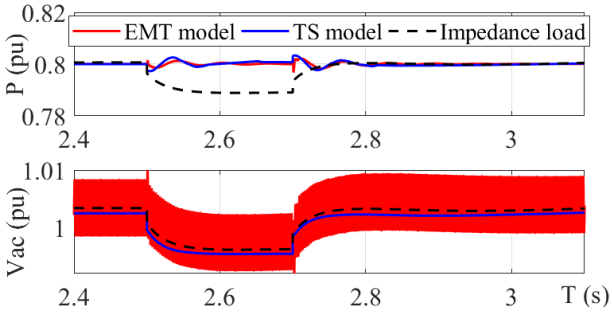

Fig. 7. Transmission line disconnection between Bus 7 and 8.

TABLE I. Load profile at Bus 5,6 and 8.

Bus	Load type	Active Power (MW)	Reactive Power (MVA)
5	dynamic EV charger	80	0
5	constant impedance	45	50
6	constant impedance	90	30
8	constant impedance	100	35

A. Transmission Line Disconnection

As illustrated in Fig. 6, one of the transmission line between Bus 7 and Bus 8 is tripped to evaluate the load model performance during small grid disturbance.The transmission line is tripped at t = 2.5 s and lasts for 0.2 s. The active power consumption P and the AC voltage V_{ac} at terminal Bus 5. Simulation results are illustrated in Fig. 7, where red curves illustrate the EMT model, and blue curves illustrate the proposed TS model. It can be observed that the dynamic performance of the proposed EV charging load presents a good match with that of the equivalent EMT load model.

The comparison case in TSAT, where the proposed EV charger model is replaced by the equivalent constant impedance load at Bus 5, is illustrated by black dash curves in Fig. 7. It can be observed that the static load cannot represent the dynamic performance of the P compared with the proposed dynamic load model.

B. Ground Fault Remote from the EV Charging Unit

A three-phase ground fault at Bus 8 is applied to evaluate the load model performance during grid contingency. The LVRT control is applied to the EV charger to withstand the low terminal voltage. The Bus 8 is grounded with admittance at t = 2.5 s and lasts for 0.2 s. The dynamic performance of the EV charger AC and DC side model are both evaluated, where the following variables are recorded respectively: P, V_{ac} and the DC-link voltage V_{dc} across the energy storage device C_{ev}. Simulation results are illustrated in Fig. 8(a). Both the ac side and DC side performance of the TS model achieve a good match with that of the EMT model. The simulation results in TSAT with equivalent constant impedance load at Bus 5 also validate that the proposed EV charger load can reflect the dynamic performance more accurately at system transients.

C. Ground Fault Close to the Terminal of EV Charging Unit

In this case, a three-phase ground fault is applied at Bus 5 where the EV charger load is directly connected to, so the ground fault influences the EV charger load more severely compared with the last case. The simulation results are illustrated in Fig. 8(b), and compared with those of PSCAD/EMTDC models, it is observed that the performance of the proposed EV charging model achieves a relatively good match with that of the EMT model. Similar to last case, simulation results with the equivalent constant impedance load are different from that of with the proposed dynamic load model at system transients.

V. Conclusion

In this paper, an electromechanical model for a fast EV charging unit is proposed and developed in TSAT, which is suitable for large-scale power system dynamic analysis. The EV charger model is based on the PE converter average model, as well as reasonable simplification on the battery load dynamics and controller dynamics. Additionally, the LVRT control is integrated into the model to present a more practical dynamic performance during a grid contingency. The accuracy of the TS model has been validated by comparing the simulation

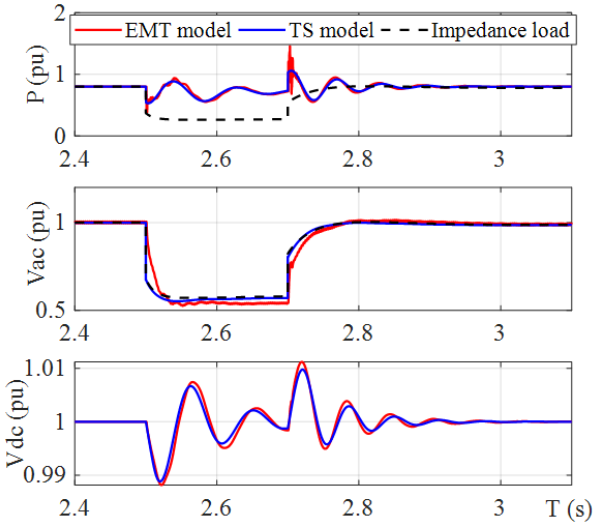

(a) EV charger model: Response to remote ground fault at Bus 8.

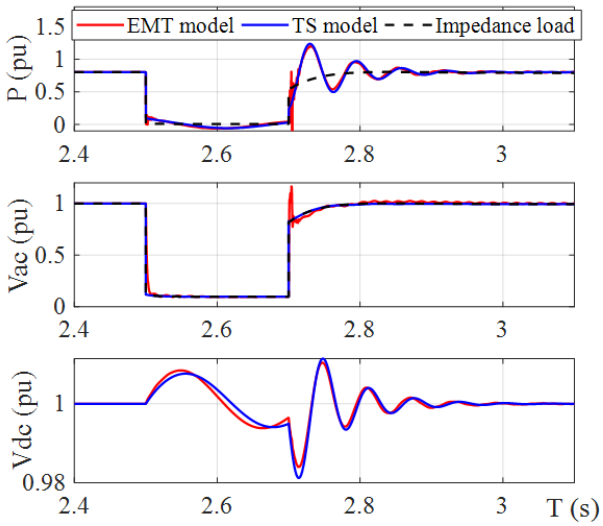

(b) EV charger model: Response to close ground fault at Bus 5.

Fig. 8. EV charger model subject to the three-phase ground fault at Bus 8 and Bus 5: active power, AC terminal voltage and DC-link voltage.

results with those of the PSCAD/EMTDC model subject to the transmission line disconnection and three-phase ground fault. According to the simulation results, the fast EV charger model developed in TSAT can accurately reflect the dynamic performance regarding the electromechanical transients.

ACKNOWLEDGMENT

This work was supported primarily by the Engineering Research Center Program of the National Science Foundation and the Department of Energy under NSF Award Number EEC-1041877 and the CURENT Industry Partnership Program.

REFERENCES

[1] D. Mao, D. Meyer, and J. Wang, "Evaluating pev's impact on long-term cost of grid assets," in *IEEE Power & Energy Society Innovative Smart Grid Technologies Conference (ISGT)*, 2017, pp. 1–5.

[2] A. Arif, Z. Wang, J. Wang, B. Mather, H. Bashualdo, and D. Zhao, "Load modeling—a review," *IEEE Transactions on Smart Grid*, vol. 9, no. 6, pp. 5986–5999, 2017.

[3] K. Yamashita, S. M. Villanueva, and J. Milanovic, "Initial results of international survey on industrial practice on power system load modelling conducted by cigre wg c4. 605," in *Proc. CIGRE Symp.*, vol. 4, 2011.

[4] J. V. Milanovic, K. Yamashita, S. M. Villanueva, S. Ž. Djokic, and L. M. Korunović, "International industry practice on power system load modeling," *IEEE Transactions on Power Systems*, vol. 28, no. 3, pp. 3038–3046, 2012.

[5] H. Saad, J. Peralta *et al.*, "Dynamic averaged and simplified models for MMC-based HVDC transmission systems," *IEEE transactions on Power delivery*, vol. 28, no. 3, pp. 1723–1730, 2013.

[6] S. Wang, E. Farantatos, and K. Tomsovic, "Wind turbine generator modeling considerations for stability studies of weak systems," in *North American Power Symposium (NAPS)*, 2017, pp. 1–6.

[7] P. Shamsi and B. Fahimi, "Dynamic behavior of multiport power electronic interface under source/load disturbances," *IEEE Transactions on Industrial Electronics*, vol. 60, no. 10, pp. 4500–4511, 2012.

[8] W. Jiang and B. Fahimi, "Multiport power electronic interface—concept, modeling, and design," *IEEE Transactions on Power Electronics*, vol. 26, no. 7, pp. 1890–1900, 2010.

[9] M. Restrepo, J. Morris, M. Kazerani, and C. A. Canizares, "Modeling and testing of a bidirectional smart charger for distribution system EV integration," *IEEE Transactions on Smart Grid*, vol. 9, no. 1, pp. 152–162, 2016.

[10] X. Liang, "Linearization approach for modeling power electronics devices in power systems," *IEEE Journal of Emerging and Selected Topics in Power Electronics*, vol. 2, no. 4, pp. 1003–1012, 2014.

[11] X. Liang and J. He, "Load model for medium voltage cascaded H-bridge multi-level inverter drive systems," *IEEE Power and Energy Technology Systems Journal*, vol. 3, no. 1, pp. 13–23, 2016.

[12] Y. Liu, V. Vittal, and J. Undrill, "Performance-based linearization approach for modeling induction motor drive loads in dynamic simulation," *IEEE Transactions on Power Systems*, vol. 32, no. 6, pp. 4636–4643, 2017.

[13] D. Ramasubramanian and V. Vittal, "Positive sequence induction motor speed control drive model for time-domain simulations," *IET Generation, Transmission & Distribution*, vol. 11, no. 7, pp. 1809–1819, 2017.

[14] D. Ramasubramanian, "Impact of converter interfaced generation and load on grid performance," Ph.D. dissertation, Arizona State University, Arizona, May 2017.

[15] R. Adams, B.Badrzadeh, and M. Barbieri, "Modeling of inverter based generation for power system dynamic studies," CIGRE/ CIRED, Tech. Rep.

[16] Z. Ma, J. Xie, and Z. Wang, "Mathematical representation of the WECC composite load model," *arXiv preprint arXiv:1902.08866*, 2019.

[17] D. Mao, K. Potty, and J. Wang, "The impact of power-electronics-based load dynamics on large-disturbance voltage stability," in *IEEE Power & Energy Society General Meeting (PESGM)*, 2018, pp. 1–5.

[18] C. M. Shepherd, "Design of primary and secondary cells II. an equation describing battery discharge," *Journal of the Electrochemical Society*, vol. 112, no. 7, pp. 657–664, 1965.

[19] *Power Quality Requirements for Plug-In Electric Vehicle Chargers*, SAE International Std. J2894-1, 2019.

[20] R. Irnawan, F. da Silva, C. L. Bak, and T. Bregnhoj, "Evaluation of half-bridge modular multilevel converter model for VSC-HVDC transient stability studies," in *13th IET International Conference on AC and DC Power Transmission*, 2017, pp. 1–6.

[21] N.-T. Trinh, M. Zeller, K. Wuerflinger, and I. Erlich, "Generic model of MMC-VSC-HVDC for interaction study with ac power system," *IEEE Transactions on Power Systems*, vol. 31, no. 1, pp. 27–34, 2015.

[22] J. Freytes, L. Papangelis, H. Saad, P. Rault, T. Van Cutsem, and X. Guillaud, "On the modeling of MMC for use in large scale dynamic simulations," in *Power Systems Computation Conference (PSCC)*, 2016, pp. 1–7.

[23] S. Wang, X. Zhao, F. Xue, W. Li, H. Peng, D. Shi, S. Wang, and Z. Wang, "Electromechanical transient modeling of modular multilevel converter based HVDC network," in *IEEE Sustainable Power Energy Conference*, 2019.